2026 IEEE Intelligent Vehicles Symposium (IV)
June 22-25, 2026. Detroit, MI, USA

Negotiation-Based Conflict Resolution for Connected Automated Vehicles in Mixed Traffic

Kai Deng, Sergei S. Avedisov, Takayuki Shimizu, Onur Altintas, and Gábor Orosz

2026 IEEE Intelligent Vehicles Symposium (IV) | 979-8-3315-4793-6/26/$31.00 ©2026 IEEE | DOI: 10.1109/IV66570.2026.11623846

***Abstract*—A negotiation-based cooperative maneuvering strategy is proposed to resolve conflicts in mixed traffic scenarios, where connected automated vehicles (CAVs) coexist with connected human-driven vehicles (CHVs). We characterize the interactions between the vehicles using private and interactive logical propositions. Conflict analysis is performed to determine the conditions under which a CAV should send a negotiation request. A reachability-based response mechanism is formulated to enable CAVs to respond to incoming negotiation requests. Simulation studies utilizing real vehicle data demonstrate that the proposed strategy improves time efficiency while guaranteeing conflict free maneuvering. To the best of our knowledge, this study is the first to implement decentralized negotiation among CAVs with explicit consideration of the surrounding CHVs in mixed traffic scenarios.**

I. Introduction

Conflicts in traffic can occur when multiple vehicles attempt to utilize the same road resources at unsignalized intersections, roundabouts, and during lane-changes [1]. Mismanagement of these conflicts can lead to safety hazards and reduce the traffic efficiency [2]. With the advancement of wireless vehicle-to-everything (V2X) communication, connected automated vehicles (CAVs) offer new opportunities to cooperatively resolve conflicts in complex traffic scenarios [3]. Status and intent information obtained from other vehicles can be leveraged by CAVs [4], but solely relying on these may lead to suboptimal decision-making. Centralized cooperation may be used to coordinate CAVs [5], but this requires the controllability of all traffic participants [6], which limits its applicability.

Negotiation can lead to an explicit agreement between CAVs, which offers a new mechanism for conflict resolution, enabling them to actively request future road resources and respond to such requests [7], [8]. Existing negotiation-based methods often lack clear criteria for determining the feasibility of conflict resolution and the appropriate timing for sending negotiation requests [9], [10]. Most approaches also assume that all traffic participants are automated [11]–[13]. In contrast, mixed traffic scenarios, where vehicles with varying levels of automation and cooperation coexist, are expected to dominate in the foreseeable future, highlighting the importance of developing negotiation strategies suitable for such scenarios.

Kai Deng and Gábor Orosz are with the Department of Mechanical Engineering, University of Michigan, Ann Arbor, MI 48109, USA, {kaideng, orosz}@umich.com.

Sergei S. Avedisov, Takayuki Shimizu, and Onur Altintas are with Toyota Motor North America R&D - InfoTech Labs, Mountain View, CA 94043, USA. {sergei.avedisov, takayuki.shimizu, onur.altintas}@toyota.com.

Gábor Orosz is also with the Department of Civil and Environmental Engineering, University of Michigan, Ann Arbor, MI 48109, USA.

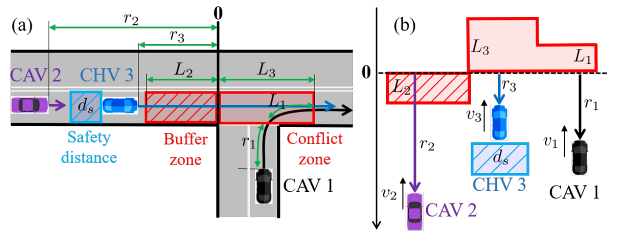

Fig. 1. (a) Conflict scenario at an unsignalized intersection. (b) Simplified mathematical model used for negotiation in the mixed traffic scenarios.

To address the above challenges, we propose a novel negotiation strategy. We first formulate conflicts in mixed traffic by considering CAV-CHV and CAV-CAV interactions using private and interactive propositions, respectively. From the perspective of requesters, the feasibility of negotiation is determined using a conflict analysis, which also determines the timing of sending negotiation requests. From the perspective of the responders, reachability analysis is utilized to guide decision-making and generate responses. The performance of the proposed negotiation strategy is evaluated through simulations utilizing real vehicle data. The results demonstrate that negotiation creates new opportunities for conflict resolution, while improving time efficiency and guaranteeing conflict-free maneuvering in mixed traffic.

II. Problem Formulation

The scenario in Fig. 1(a) is utilized to illustrate potential conflicts in mixed traffic. Here CAV 2 and CHV 3 are driving on the main road while CAV 1 wants to merge between them. Fig. 1(b) depicts a simplified model that can be used to describe this scenario and can also be applied to a large set of scenarios with different road configurations. We assume that all vehicles are able to share status (i.e., position and velocity) and intent (i.e., bounds of velocity and acceleration) [4], while the negotiation is performed exclusively between the CAVs. The interaction between a CAV and the CHV is characterized using a so-called private proposition, while an interactive proposition is employed to describe CAV-CAV interactions. Since there are two CAVs involved, each of them may have a different perspective on how to resolve conflicts.

We begin by describing the conflict from the perspective of CAV 1. The conflict zone (red) and buffer zone (red hatched) are illustrated in Fig. 1(a). Accordingly, a conflict-free maneuver is defined as follows: when CAV 1 enters the conflict zone, CHV 3 must have already cleared the conflict zone, and CAV 2 must not have entered the buffer zone yet.

This way, CAV 1 can keep safe distances from both CAV 2 and CHV 3 when entering the conflict zone. For the CAVs, the CHV serves as the environment whose behavior cannot be controlled. In contrast, CAVs may interact with each other and negotiate for road resources.

The conflict-free maneuver between CAV 1 and CHV 3 can be mathematically formulated via the private proposition

$$\mathcal{P}_1 := \{\exists t > 0, (r_1(t) = 0) \wedge (r_3(t) \leq -(L_3 + l_3))\}. \quad (1)$$

Moreover, the conflict-free maneuver between CAV 1 and CAV 2 can be formulated as the interactive proposition

$$\mathcal{I} := \{\exists t > 0, (r_1(t) = 0) \wedge (r_2(t) \geq L_2)\}. \quad (2)$$

Here r_1, r_2, and r_3 denote the positions of the vehicles relative to the conflict zone, see Fig. 1. The path lengths of traveling through the conflict and buffer zones are denoted by L_1, L_2, and L_3. Lastly, l_3 denotes the length of the CHV 3. As will be shown later, r_1, r_2, and r_3 decrease monotonically in time t. Thus, we can rewrite the propositions $\mathcal{P}_1$ and $\mathcal{I}$ as

$$\mathcal{P}_1^\dagger := \{\exists t_{1,\mathrm{in}}, \exists t_{3,\mathrm{out}}, t_{1,\mathrm{in}} \geq t_{3,\mathrm{out}}\}, \quad (3)$$

$$\mathcal{I}^\dagger := \{\exists t_{1,\mathrm{in}}, \exists t_{2,\mathrm{in}}, t_{1,\mathrm{in}} \leq t_{2,\mathrm{in}}\}, \quad (4)$$

where $t_{1,\mathrm{in}}$ denotes the time when CAV 1 enters the conflict zone, $t_{3,\mathrm{out}}$ is the time when CHV 3 exits the conflict zone, and $t_{2,\mathrm{in}}$ is the time when CAV 2 enters the buffer zone. These are defined by $r_1(t_{1,\mathrm{in}}) = 0$, $r_3(t_{3,\mathrm{out}}) = -(L_3 + l_3)$, $r_2(t_{2,\mathrm{in}}) = L_2$, respectively. In summary, a conflict-free maneuver for CAV 1 is given by the proposition

$$\mathcal{M}_1 := \mathcal{I}^\dagger \wedge \mathcal{P}_1^\dagger. \quad (5)$$

Similarly, CAV 2 has two objectives. It needs to maintain a safe distance from CHV 3 until CAV 2 enters the conflict zone, which can be formulated as the private proposition

$$\mathcal{P}_2 := \{\forall t \in (0, t_{2,\mathrm{in}}], r_2(t) - r_3(t) - l_3 \geq d_\mathrm{s}\}, \quad (6)$$

where d_s indicates the safety distance. Also, CAV 2 needs to ensure that it does not enter the buffer zone before the CAV 1 enters the conflict zone. This is defined by the interactive proposition (2), or alternatively by (4). Then, for CAV 2, a conflict-free maneuver is given by the proposition

$$\mathcal{M}_2 := \mathcal{I}^\dagger \wedge \mathcal{P}_2. \quad (7)$$

To describe the longitudinal dynamics of the vehicles, we use the positions r_1, r_2, r_3 and velocities as v_1, v_2, v_3, see Fig. 1. Defining the states $x_i = [r_i, v_i]^\top$ and considering the accelerations as the inputs u_i, the dynamics are given by

$$\dot{x}_i = f_i(x_i, u_i) = Ax_i + Bu_i, \quad i = 1, 2, 3, \quad (8)$$

where

$$A = \begin{bmatrix} 0 & -1 \\ 0 & 0 \end{bmatrix}, \quad B = \begin{bmatrix} 0 \\ 1 \end{bmatrix}, \quad (9)$$

$x = [x_1^\top, x_2^\top, x_3^\top]^\top = [r_1, v_1, r_2, v_2, r_3, v_3]^\top \in \Omega$, and $u = [u_1, u_2, u_3]^\top \in \Upsilon$, that is, the states and the input are assumed to be within the bounded domains

$$\begin{aligned} \Omega = [-(L_1 + l_1), \infty) \times [v_1^{\min}, v_1^{\max}] \times [-(L_2 + l_2), \infty) \\ \times [v_2^{\min}, v_2^{\max}] \times [-(L_3 + l_3), \infty) \times [v_3^{\min}, v_3^{\max}], \\ \Upsilon = [a_1^{\min}, a_1^{\max}] \times [a_2^{\min}, a_2^{\max}] \times [a_3^{\min}, a_3^{\max}]. \end{aligned} \quad (10)$$

It is worth noting that the proposed method can generalize to other traffic scenarios involving conflicts, such as roundabouts and intersections [14], provided that the conflict zone, buffer zone, and safety distances are properly defined. To ensure conflict-free maneuvers from the perspectives of both CAVs, below we present a negotiation-based cooperation strategy which guarantees that propositions $\mathcal{M}_1$ and $\mathcal{M}_2$ hold.

III. Negotiation in Mixed Traffic

In this section, a request-response negotiation protocol is established to resolve conflicts. Performing conflict analysis from its own perspective, the requester (CAV 1) determines whether cooperation from CAV 2 is required to merge between CAV 2 and CHV 3 without conflict, and it sends a negotiation request to CAV 2. Then the responder (CAV 2), sends a response to CAV 1 based on the conflict analysis performed from its own perspective. Once CAV 1 and CAV 2 reach an agreement, each of them applies its own controller in a decentralized manner to execute the maneuver without conflict. Note that our negotiation protocol is able to deal with the mixed traffic scenarios with both CAVs and CHVs present.

A. Negotiation from the perspective of requester

The negotiation starts when CAV 1 sends a request to CAV 2. The timing of the request plays a crucial role: initiating the negotiation too early may result in unnecessary maneuvers and increased communication load, while a delayed request can make conflict resolution challenging, or even infeasible. We show that the propositions above can be used to determine the appropriate timing.

From the perspective of CAV 1, based on the Proposition $\mathcal{M}_1$ given in (5), the state space Ω can be partitioned into four disjoint regions considering the current states x and future control inputs u_i of the vehicles:

$$\begin{aligned} \mathcal{M}_1^\mathrm{b} &:= \{x \in \Omega | \forall u_1, \forall u_2, \forall u_3, \mathcal{M}_1\}, \\ \mathcal{M}_1^\mathrm{g} &:= \{x \in \Omega | (\exists u_1, \forall u_2, \forall u_3, \mathcal{M}_1) \wedge \\ &\qquad \neg(\forall u_1, \forall u_2, \forall u_3, \mathcal{M}_1)\}, \\ \mathcal{M}_1^\mathrm{y} &:= \{x \in \Omega | (\exists u_1, \exists u_2, \exists u_3, \mathcal{M}_1) \wedge \\ &\qquad \neg(\exists u_1, \forall u_2, \forall u_3, \mathcal{M}_1)\}, \\ \mathcal{M}_1^\mathrm{r} &:= \{x \in \Omega | \forall u_1, \forall u_2, \forall u_3, \neg\mathcal{M}_1\}. \end{aligned} \quad (11)$$

The symbol $\neg$ means negation. In region $\mathcal{M}_1^\mathrm{b}$, no conflict can occur regardless of the control strategies adopted by CAV 1, CAV 2, or CHV 3. In region $\mathcal{M}_1^\mathrm{g}$, there exists a control strategy for CAV 1 to merge between CAV 2 and CHV 3 without conflict for all control strategies of CAV 2 and CHV 3. Therefore, for $x \in \mathcal{M}_1^\mathrm{b} \cup \mathcal{M}_1^\mathrm{g}$, negotiation is not necessary, since CAV 1 can avoid conflict without cooperating with CAV 2. In region $\mathcal{M}_1^\mathrm{y}$, for specific actions of CAV 1, CAV 2, and CHV 3, a conflict-free maneuver may be achieved. Note that CHV 3's action cannot be assigned (since it is not an automated vehicle). Thus, conflicts may only be resolved through negotiation between CAV 1 and CAV 2 in part of the region $\mathcal{M}_1^{\mathrm{y}}$. In region $\mathcal{M}_1^{\mathrm{r}}$ no control strategies exist to achieve a conflict-free maneuver. Therefore, negotiation is not necessary if $x \in \mathcal{M}_1^{\mathrm{r}}$. One can prove that $\Omega = \mathcal{M}_1^{\mathrm{b}} \cup \mathcal{M}_1^{\mathrm{g}} \cup \mathcal{M}_1^{\mathrm{y}} \cup \mathcal{M}_1^{\mathrm{r}}$. The subscripts b, g, y, and r denote the black, green, yellow, and red colors that are used to visualize the regions in Fig. 3.

In order to check whether the state of the system is located in a given region, we utilize the definitions

$$\begin{aligned} \Gamma_{\mathrm{ego}} &:= \{t_{1,\mathrm{in}} > 0 | T_{1,\mathrm{in}}^{\min} \le t_{1,\mathrm{in}} \le T_{1,\mathrm{in}}^{\max}\}, \\ \Gamma_{\mathrm{env}}^1 &:= \{t_{1,\mathrm{in}} > 0 | T_{3,\mathrm{out}}^{\max} \le t_{1,\mathrm{in}} \le T_{2,\mathrm{in}}^{\min}\}, \\ \Gamma_{\mathrm{env}}^2 &:= \{t_{1,\mathrm{in}} > 0 | T_{3,\mathrm{out}}^{\min} \le t_{1,\mathrm{in}} \le T_{2,\mathrm{in}}^{\max}\}, \end{aligned} \tag{12}$$

where

$$\begin{aligned} T_{1,\mathrm{in}}^{\max} &= F_{1,\mathrm{in}}(a_1^{\min}), \quad T_{1,\mathrm{in}}^{\min} = F_{1,\mathrm{in}}(a_1^{\max}), \\ T_{2,\mathrm{in}}^{\max} &= F_{2,\mathrm{in}}(a_2^{\min}), \quad T_{2,\mathrm{in}}^{\min} = F_{2,\mathrm{in}}(a_2^{\max}), \\ T_{3,\mathrm{out}}^{\max} &= F_{3,\mathrm{out}}(a_3^{\min}), \quad T_{3,\mathrm{out}}^{\min} = F_{3,\mathrm{out}}(a_3^{\max}). \end{aligned} \tag{13}$$

Here $F_{1,\mathrm{in}}(\cdot)$ gives the time when CAV 1 enters the conflict zone, $F_{2,\mathrm{in}}(\cdot)$ gives the time when CAV 2 enters the buffer zone, and $F_{3,\mathrm{out}}(\cdot)$ gives the time when CAV 3 clears the conflict zone. The detailed analytical expressions of the functions are omitted here due to space limitations. Please refer to [15] for more details.

The set Γ_{ego} represents CAV 1's acceleration capability, defined through the feasible time interval of $t_{1,\mathrm{in}}$ as shown in Fig. 2(a). The sets Γ_{env}^1 and Γ_{env}^2 represent environmental constraints introduced by other vehicles under the worst-case and best-case scenarios, respectively. In the worst case, CAV 2 and CHV 3 use maximal and minimal acceleration to reduce their gap, see Fig. 2(b). In the best case, they use minimal and maximal acceleration to increase their gap, see Fig. 2(c). Based on (12), we have the following theorem.

Theorem 1: Given the dynamics (8), the current state x, and the bounds $v_i^{\min}$, $v_i^{\max}$, $a_i^{\min}$, $a_i^{\max}$, we have

$$x \in \mathcal{M}_1^{\mathrm{b}} \Leftrightarrow \Gamma_{\mathrm{ego}} \subseteq \Gamma_{\mathrm{env}}^1, \tag{14a}$$

$$x \in \mathcal{M}_1^{\mathrm{g}} \Leftrightarrow (\Gamma_{\mathrm{ego}} \cap \Gamma_{\mathrm{env}}^1 \neq \emptyset) \wedge \neg(\Gamma_{\mathrm{ego}} \subseteq \Gamma_{\mathrm{env}}^1), \tag{14b}$$

$$x \in \mathcal{M}_1^{\mathrm{y}} \Leftrightarrow (\Gamma_{\mathrm{ego}} \cap \Gamma_{\mathrm{env}}^2 \neq \emptyset) \wedge \neg(\Gamma_{\mathrm{ego}} \cap \Gamma_{\mathrm{env}}^1 \neq \emptyset), \tag{14c}$$

$$x \in \mathcal{M}_1^{\mathrm{r}} \Leftrightarrow (\Gamma_{\mathrm{ego}} \cap \Gamma_{\mathrm{env}}^2 = \emptyset). \tag{14d}$$

The proof can be found in Appendix A.

Based on Theorem 1, the four disjoint regions are identified in the (r_1, r_2, r_3)-space for a given set of velocities, as illustrated in Fig. 3(a). The black, green and yellow regions are colored, while the red region (which is the complement of the union of the other three) is not colored to enhance the readability. Note that without negotiation, conflict cannot be avoided in the yellow region since CAV 2 and CHV 3 are uncontrollable from the perspective of CAV 1. In this case, a conflict free maneuver is only feasible when $x \in \mathcal{M}_1^{\mathrm{b}} \cup \mathcal{M}_1^{\mathrm{g}}$.

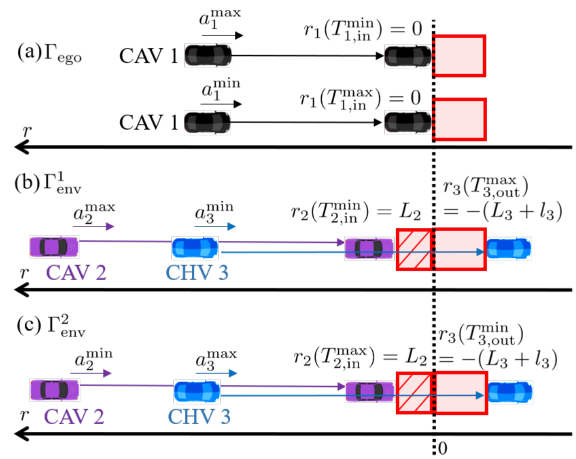

Fig. 2. Illustration of the sets defined in (12). (a) Γ_{ego} denotes the capability of CAV 1. (b) Γ_{env}^1 denotes that worst-case scenario of the environment. (c) Γ_{env}^2 denotes the best-case scenario of the environment.

Considering that CAV 3 is uncontrollable, we define the negotiable region

$$\begin{aligned} \mathcal{M}_{1,\mathrm{n}}^{\mathrm{y}} := \{x \in \Omega | (\exists u_1, \exists u_2, \forall u_3, \mathcal{M}_1) \wedge \\ \neg(\exists u_1, \forall u_2, \forall u_3, \mathcal{M}_1)\}, \end{aligned} \tag{15}$$

where control strategies exist for CAV 1 and CAV 2 to avoid conflict considering all possible actions of CHV 3. In this region, by establishing cooperation between CAV 1 and CAV 2 through negotiation, conflict-free maneuvering may be achieved. Therefore, CAV 1 should send a negotiation request to CAV 2 when $x \in \mathcal{M}_{1,\mathrm{n}}^{\mathrm{y}}$. Notice that $\mathcal{M}_{1,\mathrm{n}}^{\mathrm{y}} \subseteq \mathcal{M}_1^{\mathrm{y}}$ since the set $\{x \in \Omega | (\exists u_1, \exists u_2, \forall u_3, \mathcal{M}_1)\}$ in the definition of $\mathcal{M}_{1,\mathrm{n}}^{\mathrm{y}}$ is a subset of $\{x \in \Omega | (\exists u_1, \exists u_2, \exists u_3, \mathcal{M}_1)\}$ in the definition of $\mathcal{M}_1^{\mathrm{y}}$. The following theorem provides criteria to check whether a certain state is located in the region $\mathcal{M}_{1,\mathrm{n}}^{\mathrm{y}}$.

Theorem 2: Given the dynamics (8), the current state x, and the bounds $v_i^{\min}$, $v_i^{\max}$, $a_i^{\min}$, $a_i^{\max}$, we have

$$x \in \mathcal{M}_{1,\mathrm{n}}^{\mathrm{y}} \Leftrightarrow (\Gamma_{\mathrm{ego}} \cap \Gamma_{\mathrm{env}}^3 \neq \emptyset) \wedge \neg(\Gamma_{\mathrm{ego}} \cap \Gamma_{\mathrm{env}}^1 \neq \emptyset), \tag{16}$$

where the set

$$\Gamma_{\mathrm{env}}^3 := \{t_{1,\mathrm{in}} > 0 | T_{3,\mathrm{out}}^{\max} \le t_{1,\mathrm{in}} \le T_{2,\mathrm{in}}^{\max}\}, \tag{17}$$

correspond to the case where CAV 2 adopts the best control strategy while CHV 3 adopts the worst control strategy.

Since the structure of (17) is similar to that of (14c), its proof follows the same structure, see Appendix A for details.

Based on Theorem 2, the negotiable region can be visualized by the brown region in the (r_1, r_2, r_3)-space in Fig. 3(b). Compared to Fig. 3(a), where the initial states that allow CAV 1 to avoid conflict are limited to $\mathcal{M}_1^{\mathrm{b}} \cup \mathcal{M}_1^{\mathrm{g}}$, employing negotiation increases the feasible set to $\mathcal{M}_1^{\mathrm{b}} \cup \mathcal{M}_1^{\mathrm{g}} \cup \mathcal{M}_{1,\mathrm{n}}^{\mathrm{g}}$. Thus, negotiation provides additional opportunities to achieve conflict-free maneuvering. The intersection $\Gamma_{\mathrm{ego}} \cap \Gamma_{\mathrm{env}}^3$ in (16) represents the feasible time interval for $t_{1,\mathrm{in}}$ that allows conflict-free merge for CAV 1. Therefore, when $x \in \mathcal{M}_{1,\mathrm{n}}^{\mathrm{y}}$, CAV 1 should send a request, indicating its intention to enter the conflict zone within this time interval.

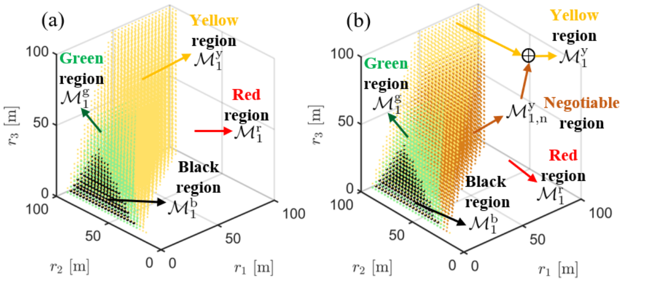

Fig. 3. Results of conflict analysis from the perspective of CAV 1 in the (r_1, r_2, r_3)-space for $v_1 = 6$ [m/s], $v_2 = 13$ [m/s], and $v_3 = 12$ [m/s], (a) without negotiation and (b) with negotiation. Here, we use constant bounds $a_i^{\min} = -3$ [m/s^2], $a_i^{\max} = 2$ [m/s^2], $v_1^{\min} = 6$ [m/s], $v_{2,3}^{\min} = 10$ [m/s], $v_i^{\max} = 15$ [m/s], $L_i = 10$ [m], and $l_i = 5$ [m].

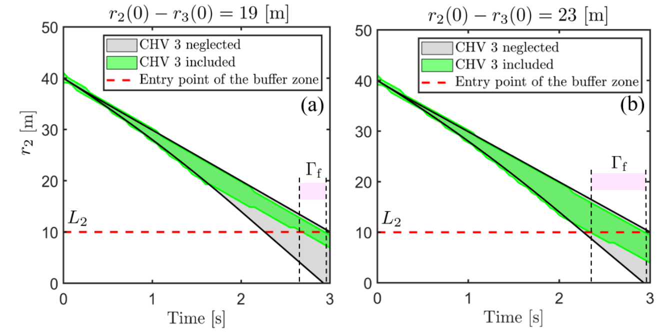

Fig. 4. (a) Forward reachable set of CAV 2 when $r_2(0) - r_3(0) = 19$ [m]. (b) Forward reachable set of CAV 2 when $r_2(0) - r_3(0) = 23$ [m]. The time step is 0.1 [s] and for other parameters of CAV 2 and CHV 3, please refer to the caption of Fig. 3.

B. Negotiation from the perspective of responder

From the perspective of CAV 2, proposition $\mathcal{M}_2$ given in (7) needs to be satisfied. One may divide the state space Ω similar to (11), but in this case, it is difficult to determine the best-case and worst-case behaviors, which were exploited in Theorems 1 and 2. Thus, we handle the private proposition $\mathcal{P}_2$ and the interactive proposition $\mathcal{I}^{\dagger}$ separately. We utilize reachability analysis to tackle the private proposition and take into account the suggestion $\Gamma_{\mathrm{ego}} \cap \Gamma_{\mathrm{env}}^3$ sent by CAV 1 to deal with the interactive proposition.

Let us consider the condition $t_{1,\mathrm{in}} \le t_{2,\mathrm{in}}$ in the interactive proposition $\mathcal{I}^{\dagger}$ defined in (4). Based on the request sent by CAV 1, $t_{1,\mathrm{in}} \in \Gamma_{\mathrm{ego}} \cap \Gamma_{\mathrm{env}}^3$, whereas the range for $t_{2,\mathrm{in}}$ is initially unknown due to the influence of CHV 3 ahead of CAV 2 (see the private proposition $\mathcal{P}_2$). We compute the feasible range for $t_{2,\mathrm{in}}$ using the forward reachability set (FRS) of CAV 2. This is defined as the set of states $x_2 \in \mathbb{R}^2$ the dynamics (8) can reach at time $t > 0$ from an initial set $\mathcal{G}_0 \subset \mathbb{R}^2$, while avoiding the time-varying collision set $\mathcal{C} \subset \mathbb{R}^2$ imposed by CHV 3. Mathematically, the FRS is defined as

$$\begin{aligned}\mathcal{R}(t) = \{y | \forall u_2 \in [u_2^{\min}, u_2^{\max}], \zeta_2(t; x_2^0, u_2(\cdot)) = y,\\ x_2^0 \in \mathcal{G}_0, \forall t^* \in [0, t], \zeta_2(t^*; x_2^0, u_2(\cdot)) \notin \mathcal{C}\},\end{aligned} \tag{18}$$

where ζ_2 denotes the general solution of

$$\frac{\mathrm{d}}{\mathrm{d}t}\zeta_2(t; x_2^0, u_2(\cdot)) = f_2\big(\zeta_2(t; x_2^0, u_2(\cdot)), u_2(t)\big), \tag{19}$$

considering initial conditions x_2^0 and historical input profiles $u_2(\cdot)$, such that $\zeta_2(0; x_2^0, u_2(\cdot)) = x_2^0$. The initial set $\mathcal{G}_0$ is defined as a small region encompassing the initial states $x_2^0 = [r_2^0, v_2^0]^\top$ of CAV 2:

$$\mathcal{G}_0 = \{(r_2, v_2) | r_2^{\mathrm{th}} \ge |r_2 - r_2^0|, v_2^{\mathrm{th}} \ge |v_2 - v_2^0|\}, \tag{20}$$

where the tunable parameters r_2^{th} and v_2^{th} specify the size of the set. The collision set $\mathcal{C}$ is defined as the set of states where CAV 2 is within the safe distance of CHV 3:

$$\mathcal{C} = \{(r_2, v_2) | r_2 \le \underline{r}_3 + l_3 + d_{\mathrm{s}}, v_2 \in [v_2^{\min}, v_2^{\max}]\}. \tag{21}$$

Here $\underline{r}_3$ is the first component of $\zeta_3(t; x_3^0, a_3^{\min})$, that is, the position of CHV 3 derived when applying the lower bound of the acceleration.

Based on [16], [17], the FRS (18) can be obtained by solving a Hamilton–Jacobi–Bellman partial differential equation (HJB-PDE). The time evolution of the resulting forward reachable set $\mathcal{R}(t)$ is illustrated in Fig. 4 (green regions) for two different initial distances between CAV 2 and CHV 3. The gray regions represent the forward reachable sets without considering the motion of CAV 3, which can be analytically computed based on the dynamics (8). Observe that the forward reachable region of CAV 2 shrinks due to the presence of CHV 3. The red dashed horizontal lines are at position $r_2 = L_2$ and the feasible time interval for $t_{2,\mathrm{in}}$ to reach this position is defined as

$$\Gamma_{\mathrm{f}} := \left\{t > 0 | L_2 \in \mathrm{Proj}_{r_2}\mathcal{R}(t)\right\}, \tag{22}$$

where $\mathrm{Proj}_{r_2} : \mathbb{R}^2 \to \mathbb{R}$ denotes the projection operator

$$\mathrm{Proj}_{r_2}\mathcal{R}(t) := \{r_2 | (r_2, v_2) \in \mathcal{R}(t)\}. \tag{23}$$

We conclude that for $t_{2,\mathrm{in}} \in \Gamma_{\mathrm{f}}$, there exists a control strategy such that the private proposition $\mathcal{P}_2$ is satisfied.

Given the feasible time intervals $\Gamma_{\mathrm{ego}} \cap \Gamma_{\mathrm{env}}^3$ for $t_{1,\mathrm{in}}$ and Γ_{f} for $t_{2,\mathrm{in}}$, CAV 2 can make decisions based on the interactive proposition $\mathcal{I}^{\dagger}$. Namely, CAV 2 accepts CAV 1's request when $\max[\Gamma_{\mathrm{ego}} \cap \Gamma_{\mathrm{env}}^3] \le \min[\Gamma_{\mathrm{f}}]$, since $t_{1,\mathrm{in}} \le t_{2,\mathrm{in}}$ holds for any choice of $t_{1,\mathrm{in}}$ and $t_{2,\mathrm{in}}$, see Fig. 5(a). Contrarily, CAV 2 rejects CAV 1's request when $\min[\Gamma_{\mathrm{ego}} \cap \Gamma_{\mathrm{env}}^3] < \max[\Gamma_{\mathrm{f}}]$, since $t_{1,\mathrm{in}} \le t_{2,\mathrm{in}}$ does not hold for any choice of $t_{1,\mathrm{in}}$ and $t_{2,\mathrm{in}}$, see Fig. 5(b). Finally, CAV 2 accepts CAV 1's request with a suggestion when $\Gamma_{\mathrm{ego}} \cap \Gamma_{\mathrm{env}}^3 \cap \Gamma_{\mathrm{f}} \neq \emptyset$, since there exist $t_{1,\mathrm{in}}$ and $t_{2,\mathrm{in}}$, such that $t_{1,\mathrm{in}} \le t_{2,\mathrm{in}}$, see Fig. 5(c) and (d).

When CAV 2 accepts CAV 1's request with a suggestion, then $T^* \in \Gamma_{\mathrm{ego}} \cap \Gamma_{\mathrm{env}}^3 \cap \Gamma_{\mathrm{f}}$ can be selected as the suggestion sent from the responder (CAV 2) to the requester (CAV 1), indicating that the responder will enter the buffer zone after T^* while the requester should enter the conflict zone before T^*, see Fig. 5(c) and (d). In other words, CAV 1 should utilize the part the interval $\Gamma_{\mathrm{ego}} \cap \Gamma_{\mathrm{env}}^3$ before T^* and CAV 2 should utilize part of the interval Γ_{f} after T^*. Such concise suggestion can be used to coordinate CAVs' motion, and thus, reduce the uncertainties, while still giving a flexibility when resolving conflicts. Based on the suggestion, the controllers of both vehicles can be realized in a decentralized manner.

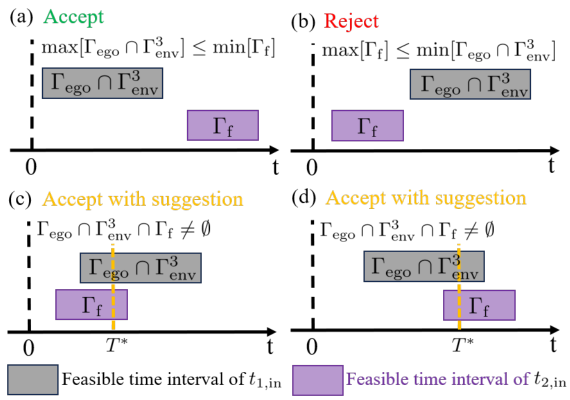

Fig. 5. Negotiation responses. Gray bars indicate the feasible time interval for $t_{1,\rm in}$, while purple bars indicate the feasible time interval for $t_{2,\rm in}$.

IV. Simulations with Real Vehicle Data

In this section, data-based simulations are utilized to verify the performance of the proposed negotiation strategy. We assume that the three connected vehicles share status and intent with other vehicles in 10 [Hz] update rate.

As in Fig. 1, CAV 2 and CHV 3 travel on the main road, while CAV 1 wants to merge between them. The velocity profiles of CAV 2 and CHV 3 are obtained when driving on a rural highway [18], [19], while the velocity of the CAV 1 is fixed at 13 $[\rm m/s]$. These are depicted in Fig. 6(a). The accelerations for CAV 2 and CHV 3 are within the bounds $[-1, 1.5]$ $[\rm m/s^2]$ while their velocities are within $[21, 27]$ $[\rm m/s]$. For CAV 1, the acceleration is within $[-2, 3]$ $[\rm m/s^2]$ and velocity is bounded by $[6, 27]$ $[\rm m/s]$. The lengths of conflict zone and buffer zone are $L_i = 10$ [m] for $i = 1, 2, 3$ while the safe distance is defined to be $d_{\rm s} = 10$ [m]. The velocity bounds are illustrated in Fig. 6(a) using blue and green shadings. The initial positions are $r_1(0) = 70$ [m], $r_2(0) = 106.7$ [m], and $r_3(0) = 80.3$ [m].

The positions of the vehicles are shown as the function of time by black, purple, and blue curves in Fig. 6(c). Here, it is assumed that the CAVs are not able to negotiate. Black, green, and yellow dots in the background highlight the regions $\mathcal{M}_1^{\rm b}$, $\mathcal{M}_1^{\rm g}$, and $\mathcal{M}_1^{\rm y}$ defined in (11) from the perspective of CAV 1. The uncolored part denotes the red region $\mathcal{M}_1^{\rm r}$. Note that these regions are shown in terms of the position r_1 of CAV 1. By applying Theorem 1, we can determine which region that CAV 1 is at. For example, at the beginning the black curve is in the yellow region $\mathcal{M}_1^{\rm y}$. Based on the analysis in Section III, without negotiation between CAV 1 and CAV 2, CAV 1 can merge between CAV 2 and CHV 3 if the system state is located in the green or black regions ($x \in \mathcal{M}_1^{\rm g} \cup \mathcal{M}_1^{\rm b}$). Then, to evaluate the benefits of negotiation, an opportunity window can be defined as the time interval when CAV 1 may achieve a conflict-free maneuver. However, in Fig. 6(c), no such opportunity exists.

In Fig. 6(b) and (d), the negotiation strategy is applied, opening a 2 [s] wide opportunity window. The colored points in the background indicate the regions according to Theorems 1 and 2. Notice that part of the yellow region $\mathcal{M}_1^{\rm y}$ becomes negotiable $\mathcal{M}_{1,\rm n}^{\rm y}$ as indicated by brown color. Correspondingly, CAV 1 should send a negotiation request to CAV 2 within this region. The response of CAV 2 is described in Subsection III-B. In this case CAV 2 always accepts CAV 1's request with a suggestion since the condition $\Gamma_{\rm ego} \cap \Gamma^3_{\rm env} \cap \Gamma_{\rm f} \neq \emptyset$ holds throughout the entire opportunity window.

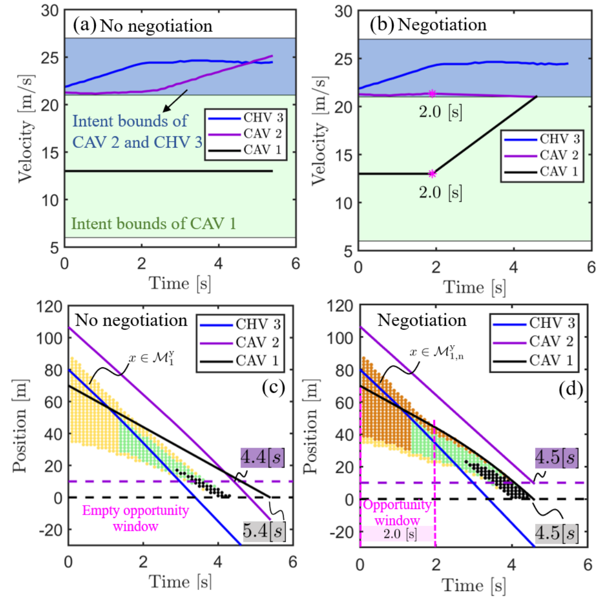

Fig. 6. Simulation results using real vehicle data. (a) Baseline velocity profiles. (b) Velocity profiles with negotiation initiated at 2.0 [s]. (c) Baseline position profiles and conflict analysis. (d) Position profiles and conflict analysis with negotiation initiated at 2.0 [s].

Fig. 6(b) and (d) also illustrate how controllers are introduced at the end of the opportunity window. In particular, the simple controllers developed in [15] are applied for CAV 1 and CAV 2 from the time moment $t = 2.0$ [s]. In order to pursue the best time efficiency, the suggestion $T^* = \min[\Gamma_{\rm ego} \cap \Gamma^3_{\rm env} \cap \Gamma_{\rm f}]$ is selected, which is the lower bound of the feasible time interval. Then the control targets for CAV 1 and CAV 2 are selected as $t_{1,\rm in} = t_{2,\rm in} = T^*$ and constant accelerations are applied to achieve these targets, see Fig. 6(b). One may notice that the black trajectory of the CAV 1 is still surrounded by brown points even after the opportunity window in Fig. 6(d). This is because applying the controllers change the behavior of CAV 1 and CAV 2, essentially further expanding the opportunity window.

As shown in Fig. 6(c), without negotiation, it takes 5.4 [s] for the CAV 1 to merge to the main road (behind CAV 2), as the behavioral uncertainties of CAV 2 and CHV 3 hinder the opportunity to merge between them. In contrast, as illustrated in Fig. 6(d), negotiation effectively eliminates this uncertainty, enabling CAV 1 to merge between CAV 2 and CHV 3 in just 4.5 [s]. Meanwhile, with negotiation, CAV 2 enters the buffer zone only 0.1 [s] later compared to the case without negotiation. These results demonstrate the advantages of negotiation in improving time efficiency while ensuring conflict-free maneuvering.

V. Conclusions

In this study we developed a maneuver coordination strategy, called negotiation, for connected automated vehicles in mixed traffic environments, where they share the road resources with connected human driven vehicles. This strategy can be applied to various scenarios, including merging, roundabout, and intersection crossing. The CAVs involved in the maneuver coordination formulated their goals and requirements through private and interactive propositions. These propositions allowed the CAVs to determine whether to seek cooperation from other vehicles through conflict analysis. If the CAV determined that cooperation was necessary to achieve a conflict-free maneuver, it sent a request to cooperate with other CAVs. The responding CAVs evaluated the received requests based on their interactive and private propositions using reachability analysis. This way they determined whether to accept, reject, or propose a suggestion in response to the cooperation request.

We conducted data-based simulations of a highway merging scenario to validate the proposed maneuver coordination strategy and compared its performance with a baseline where CAVs acted independently without explicit coordination. The results show that our negotiation strategy allows CAVs to perform the maneuver more effectively, even in the presence of non-automated vehicles. Our future work includes testing the coordination strategy with real vehicles and investigating the impact of latencies.

Appendix A
Proof of Theorem 1

For (14a), from the perspective of CAV 1, $\Gamma_{\text{ego}} \subseteq \Gamma^1_{\text{env}}$ holds. Since $\forall t_{1,\text{in}} \in \Gamma_{\text{ego}}$ always holds, then $\forall t_{1,\text{in}} \in \Gamma_{\text{ego}} \subseteq \Gamma^1_{\text{env}}$ must hold. This means that $\forall t_{1,\text{in}}$ the corresponding control strategy u_1 always leads to conflict-free cases even considering the worst-case scenario of the environment. Then $(\forall u_1, \forall u_2, \forall u_3, \mathcal{M}_1)$ must hold. So the relationship (14a) is satisfied.

For (14b), if $\Gamma_{\text{ego}} \cap \Gamma^1_{\text{env}} \neq \emptyset$ holds, then $\exists t_{1,\text{in}} \in \Gamma_{\text{ego}}$, such that $t_{1,\text{in}} \in \Gamma^1_{\text{env}}$ holds. This means that $\exists t_{1,\text{in}}$, such that the corresponding control strategy u_1 always leads to a conflict-free case considering the worst-case scenario of the environment. Then $(\exists u_1, \forall u_2, \forall u_3, \mathcal{M}_1)$ must hold. If $\neg(\Gamma_{\text{ego}} \subseteq \Gamma^1_{\text{env}})$ holds, then $\neg(\forall u_1, \forall u_2, \forall u_3, \mathcal{M}_1)$ holds according to (14a). So the relationship (14b) is satisfied.

For (14c), if $\Gamma_{\text{ego}} \cap \Gamma^2_{\text{env}} \neq \emptyset$ holds, then $\exists t_{1,\text{in}} \in \Gamma_{\text{ego}}$, such that $t_{1,\text{in}} \in \Gamma^2_{\text{env}}$ holds. This means that $\exists t_{1,\text{in}}$, such that the control strategy u_1 always leads to a conflict-free case considering the best-case scenario of the environment. Then $(\exists u_1, \exists u_2, \exists u_3, \mathcal{M}_1)$ must hold. If $\neg(\Gamma_{\text{ego}} \cap \Gamma^1_{\text{env}} \neq \emptyset)$ holds, then $\neg(\exists u_1, \forall u_2, \forall u_3, \mathcal{M}_1)$ holds according to (14a) and (14b). So the relationship (14c) is satisfied.

For (14d), if $\Gamma_{\text{ego}} \cap \Gamma^2_{\text{env}} = \emptyset$ holds, there does not exist control strategies for vehicles to avoid conflict under the best-case scenario of the environment. Then $(\forall u_1, \forall u_2, \forall u_3, \neg\mathcal{M}_1)$ always holds. So the relationship (14d) is satisfied.

References

[1] Y. Cui, S. Fang, P. Hang, and J. Sun, "A Vehicle-Infrastructure Multi-Layer Cooperative Decision-Making Framework," in *IEEE Intelligent Vehicles Symposium (IV)*, 2025, pp. 984–990.

[2] H. M. Wang, S. S. Avedisov, O. Altintas, and G. Orosz, "Intent Sharing in Cooperative Maneuvering: Theory and Experimental Evaluation," *IEEE Transactions on Intelligent Transportation Systems*, vol. 25, no. 9, pp. 12 450–12 463, 2024.

[3] Y. Liu, H. Huang, Q. Xu, S. Xu, and J. Wang, "Safer Conflict-Based Search: Risk-Constrained Optimal Pathfinding for Multiple Connected and Automated Vehicles," *IEEE Transactions on Automation Science and Engineering*, vol. 22, pp. 17 382–17 396, 2025.

[4] H. M. Wang, S. S. Avedisov, T. G. Molnár, A. H. Sakr, O. Altintas, and G. Orosz, "Conflict Analysis for Cooperative Maneuvering with Status and Intent Sharing via V2X Communication," *IEEE Transactions on Intelligent Vehicles*, vol. 8, no. 2, pp. 1105–1118, 2023.

[5] T. Mascetta, E. I. Liu, and M. Althoff, "Rule-Compliant Multi-Agent Driving Corridor Generation using Reachable Sets and Combinatorial Negotiations," in *IEEE Intelligent Vehicles Symposium (IV)*. IEEE, 2024.

[6] E. Hyeon, P. Misra, and D. Karbowski, "A Large-Scale Analysis to Optimize the Control and V2V Communication Protocols for CDA Agreement-Seeking Cooperation," *IEEE Transactions on Control Systems Technology*, vol. 33, no. 4, pp. 1333–1344, 2024.

[7] H. M. Wang, S. S. Avedisov, O. Altintas, and G. Orosz, "Negotiation in Cooperative Maneuvering using Conflict Analysis: Theory and Experimental Evaluation," in *IEEE Intelligent Vehicles Symposium (IV)*. IEEE, 2024, pp. 2297–2302.

[8] B. Haefner, V. Bajpai, J. Ott, and G. A. Schmitt, "A Survey on Cooperative Architectures and Maneuvers for Connected and Automated Vehicles," *IEEE Communications and Tutorials*, vol. 24, no. 1, pp. 380–403, 2022.

[9] D. Heß, R. Lattarulo, J. Pérez, T. Hesse, and F. Köster, "Negotiation of Cooperative Maneuvers for Automated Vehicles: Experimental Results," in *IEEE Intelligent Transportation Systems Conference (ITSC)*, 2019, pp. 1545–1551.

[10] D. Maksimovski, C. Facchi, and A. Festag, "Priority Maneuver (PriMa) Coordination for Connected and Automated Vehicles," in *IEEE Intelligent Transportation Systems Conference (ITSC)*. IEEE, 2021, pp. 1083–1089.

[11] D. Maksimovski, S. Lobo, and C. Facchi, "Prioritization of Maneuver Coordination Messages and the Impact of Decentralized Congestion Control," in *99th IEEE Vehicular Technology Conference (VTC2024-Spring)*. IEEE, 2024, pp. 1–7.

[12] K. Wang, Y. Wang, H. Du, and K. Nam, "Game-Theory-Inspired Hierarchical Distributed Control Strategy for Cooperative Intersection Considering Priority Negotiation," *IEEE Transactions on Vehicular Technology*, vol. 70, no. 7, pp. 6438–6449, 2021.

[13] W. Xu, A. Willecke, M. Wegner, L. Wolf, and R. Kapitza, "Autonomous Maneuver Coordination via Vehicular Communication," in *49th Annual IEEE/IFIP International Conference on Dependable Systems and Network Workshops (DSN-W)*. IEEE, 2019, pp. 70–77.

[14] C. Liu, C.-W. Lin, S. Shiraishi, and M. Tomizuka, "Distributed Conflict Resolution for Connected Autonomous Vehicles," *IEEE Transactions on Intelligent Vehicles*, vol. 3, no. 1, pp. 18–29, 2018.

[15] K. Deng, S. S. Avedisov, H. M. Wang, O. Altintas, and G. Orosz, "Negotiation Protocol Design for Cooperative Maneuvering of Connected Automated Vehicles using Conflict Charts," in *IEEE Intelligent Vehicles Symposium (IV)*. IEEE, 2025, pp. 2019–2024.

[16] M. Chen, S. Bansal, J. F. Fisac, and C. J. Tomlin, "Robust Sequential Trajectory Planning Under Disturbances and Adversarial Intruder," *IEEE Transactions on Control Systems Technology*, vol. 27, no. 4, pp. 1566–1582, 2019.

[17] I. A. Mitchell and J. A. Templeton, "A Toolbox of Hamilton-Jacobi Solvers for Analysis of Nondeterministic Continuous and Hybrid Systems," in *Hybrid Systems: Computation and Control*, M. Morari and L. Thiele, Eds., 2005, vol. 3414, pp. 480–494.

[18] J. I. Ge and G. Orosz, "Connected cruise control among human-driven vehicles: Experiment-based parameter estimation and optimal control design," *Transportation Research Part C*, vol. 95, pp. 445–459, 2018.

[19] G. Orosz and T. G. Molnár, *Dynamics and Control of Connected Vehicles*. Springer, 2025.